Video Article

Using Multi-fluorinated Bile Acids and *In Vivo* Magnetic Resonance Imaging to Measure Bile Acid Transport

Jessica Felton[1], Kunrong Cheng[2], Anan Said[2], Aaron C. Shang[2], Su Xu[3], Diana Vivian[4], Melissa Metry[5], James E. Polli[5], Jean-Pierre Raufman[2,6]

[1]Department of Surgery, University of Maryland School of Medicine

[2]Department of Medicine, University of Maryland School of Medicine

[3]Department of Radiology, University of Maryland School of Medicine

[4]Food and Drug Administration

[5]Department of Pharmaceutical Sciences, University of Maryland School of Pharmacy

[6]VA Maryland Health Care System

Correspondence to: Jean-Pierre Raufman at jraufman@medicine.umaryland.edu

URL: https://www.jove.com/video/54597
DOI: doi:10.3791/54597

Keywords: Medicine, Issue 117, Bile acids, magnetic resonance imaging, fluorine labeling, gallbladder, mouse, transport

Date Published: 11/27/2016

Citation: Felton, J., Cheng, K., Said, A., Shang, A.C., Xu, S., Vivian, D., Metry, M., Polli, J.E., Raufman, J.P. Using Multi-fluorinated Bile Acids and *In Vivo* Magnetic Resonance Imaging to Measure Bile Acid Transport. *J. Vis. Exp.* (117), e54597, doi:10.3791/54597 (2016).

Abstract

Along with their traditional role as detergents that facilitate fat absorption, emerging literature indicates that bile acids are potent signaling molecules that affect multiple organs; they modulate gut motility and hormone production, and alter vascular tone, glucose metabolism, lipid metabolism, and energy utilization. Changes in fecal bile acids may alter the gut microbiome and promote colon pathology including cholerrheic diarrhea and colon cancer. Key regulators of fecal bile acid composition are the small intestinal Apical Sodium-dependent Bile Acid Transporter (ASBT) and fibroblast growth factor-19 (FGF19). Reduced expression and function of ASBT decreases intestinal bile acid up-take. Moreover, *in vitro* data suggest that some FDA-approved drugs inhibit ASBT function. Deficient FGF19 release increases hepatic bile acid synthesis and release into the intestines to levels that overwhelm ASBT. Either ASBT dysfunction or FGF19 deficiency increases fecal bile acids and may cause chronic diarrhea and promote colon neoplasia. Regrettably, tools to measure bile acid malabsorption and the actions of drugs on bile acid transport *in vivo* are limited. To understand the complex actions of bile acids, techniques are required that permit simultaneous monitoring of bile acids in the gut and metabolic tissues. This led us to conceive an innovative method to measure bile acid transport in live animals using a combination of proton (^{1}H) and fluorine (^{19}F) magnetic resonance imaging (MRI). Novel tracers for fluorine (^{19}F)-based live animal MRI were created and tested, both *in vitro* and *in vivo*. Strengths of this approach include the lack of exposure to ionizing radiation and translational potential for clinical research and practice.

Video Link

The video component of this article can be found at https://www.jove.com/video/54597/

Introduction

Along with their classical role as detergents that facilitate fat absorption from the gut, bile acids have emerged as potent signaling molecules affecting multiple organs in addition to those associated with their enterohepatic circulation[1,2]. In addition to controlling their own metabolism, bile acids modulate several aspects of gastrointestinal physiology (*e.g.*, gut motility and incretin hormone production, colon physiology, and cancer susceptibility) and have systemic effects on vascular tone, glucose and lipid metabolism, and energy utilization. While some of these effects are mediated in the gut, others are due to postprandial changes in systemic bile acid levels, as noted in obese patients or after gastric by-pass surgery. To elucidate the complex metabolic actions of bile acids new technology is required that permits simultaneous monitoring of bile acid levels in different anatomical compartments, in the gastrointestinal tract and metabolic tissues (liver, pancreas, skeletal muscle and adipose). Obtaining such temporal and spatial information requires innovative technology - *in vivo* imaging using novel bile acid tracers as described here is such a novel approach.

Bile acid composition and distribution in anatomical compartments are regulated by factors that modulate their hepatic synthesis and ileal uptake, including diet, surgery, antibiotic use and changes in gut flora. A key regulator of intestinal bile acid uptake for their enterohepatic circulation[3] (**Figure 1**) is the ileal Apical Sodium-dependent Bile Acid Transporter (ASBT; *SLC10A2*). Although passive absorption occurs throughout the intestines, ASBT mediates uptake of 95% of intestinal bile acids so that normally there is limited spillage of bile acids into the feces. Asbt-deficient (*Slc10a2*$^{-/-}$) mice have increased fecal bile acids and a diminished bile acid pool[4].

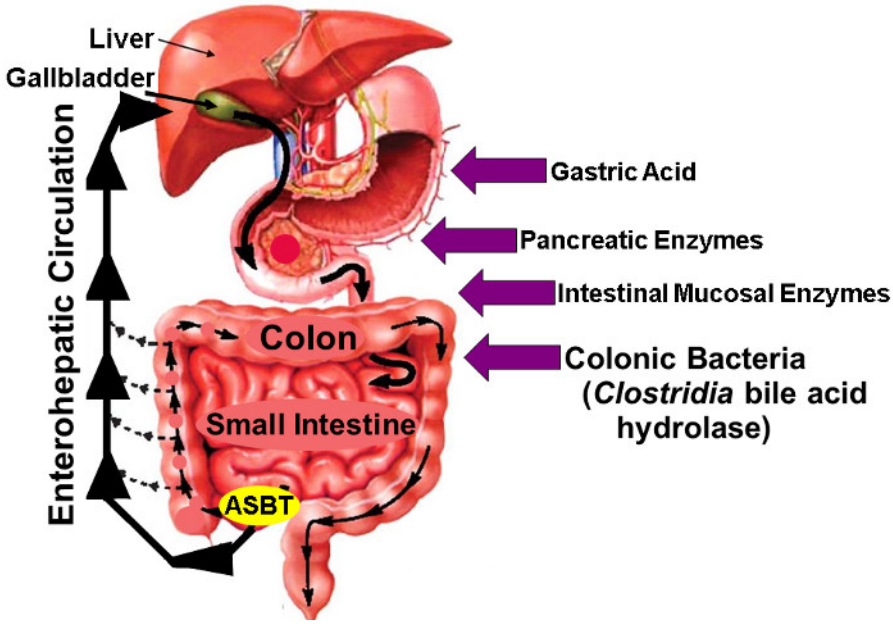

Figure 1: Enterohepatic Circulation of Bile Acids.
Illustration of Enterohepatic Circulation whereby Bile Acids are Synthesized in the Liver, Excreted into the Biliary Tree, Stored in the Gallbladder, Released into the Proximal Small Intestine with Meals, and Actively taken up *via* ASBT in the Distal Ileum. Whereas small amounts of bile acids are absorbed passively throughout the gut, approximately 95% of intestinal bile acids are transported actively by ASBT resulting in minimal (approximately 5%) loss in the stool which is compensated by a similar amount of new bile acid synthesis in the liver, thereby maintaining a steady-state bile acid pool. The arrows on the right identify factors that may impact native and fluorine-labeled bile acid stability, including gastric acid, pancreatic and intestinal mucosal enzymes, and, most importantly, hydrolytic enzymes released by *Clostridial* species that colonize the distal small bowel and colon. (Modified with permission[16]) Please click here to view a larger version of this figure.

Bile acid malabsorption can be categorized into three types, each of which increases fecal dihydroxy bile acids, thereby causing intermittent or chronic diarrhea. Type 1 results from gross ileal pathology (*e.g.,* resection, Crohn disease)[5]. Type 3 results from cholecystectomy, vagotomy, celiac disease, bacterial overgrowth, and pancreatic insufficiency. In contrast, persons with 'primary' (Type 2) bile acid malabsorption pose a formidable diagnostic challenge because they lack such antecedent conditions and do not have evidence of pathology in the ileum. Hence, primary bile acid malabsorption is commonly misdiagnosed as diarrhea-predominant irritable bowel syndrome (IBS-D), perhaps the most common reason for gastroenterology-related out-patient visits. It has been estimated that one-third of patients with IBS-D have primary bile acid malabsorption; in the U.S., this may represent several million persons[5]. Recent insights indicate that primary BAM derives from impaired feedback inhibition of hepatic bile acid synthesis by intestinal fibroblast growth factor-19 (FGF19), not from reduced expression or function of ASBT.

In primary bile acid malabsorption, low plasma levels of FGF19 fail to shut off hepatic bile acid synthesis - the resulting increase in intestinal bile acids saturates bile acid transporters, including ASBT, and the augmented spillage of bile acids into the feces causes diarrhea[6] (**Figure 2**). Mice deficient in Fgf15 (murine FGF19) have an expanded bile acid pool and increased fecal bile acids[7].

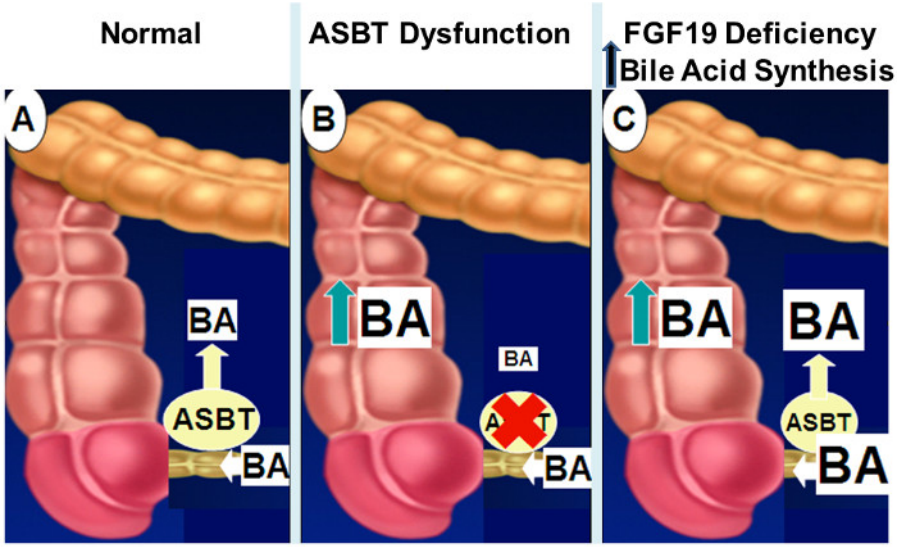

Figure 2: Mechanisms of Intestinal Bile Acid Malabsorption.
Normally, as shown in **panel A**, approximately 95% of intestinal bile acids are absorbed by active transport in the distal ileum via ASBT. When ASBT expression or activity is diminished (**panel B**), impaired intestinal bile acid uptake results in spillage of bile acids into the colon. With impaired FGF19 signaling (**panel C**), the lack of feedback inhibition of hepatic bile acid synthesis results in increased concentrations of intestinal bile acids that overwhelm ASBT transport capacity with spillage of bile acids into the colon. Please click here to view a larger version of this figure.

Long-term, chronic elevation in fecal bile acids may promote colon neoplasia. Colon neoplasia arises from progressive mucosal dysplasia associated with somatic gene mutations, but environmental factors that increase fecal bile acids may accelerate and augment this process. In rodents, increased fecal bile acids either as a consequence of exogenous administration or Asbt deficiency promote colon dysplasia and tumor formation[8-10].

Notably, provocative findings indicate that commonly-used drugs approved by the Food and Drug Administration (FDA) potently inhibit bile acid transport by ASBT *in vitro*[11]. If these drugs reduce small intestinal bile acid transport *in vivo* and increase fecal bile acid levels, the potential impact on colon pathology would be concerning. Even a small increase in colon pathology attributed to use of such a drug could have a major health impact. A toolkit which can assess the plausibility of these *in vitro* findings and epidemiologic observations would spur additional research, including post-marketing safety studies.

Despite the need, practical assays to identify people with bile acid malabsorption are lacking. Direct measurement of fecal bile acids was rejected years ago as cumbersome, impractical, and unreliable[5]. Alternative approaches include measuring retention of a radioactive selenium-labeled cholic acid derivative (^{75}SeHCAT) and plasma levels of 7α-hydroxy-4-cholesten-3-one (C4), or a therapeutic trial of bile acid binders. ^{75}SeHCAT testing has limited availability in Europe and is not FDA-approved or available for use in the U.S. Moreover, even modest radiation exposure (0.26 mSv/^{75}SeHCAT test) from diagnostic testing raises concerns, and bacterial overgrowth and advanced liver disease may confound ^{75}SeHCAT results. C4 testing is potentially attractive since only plasma is required, but it has low positive-predictive value and testing is not widely available. Measuring serum levels of FGF19 has similar limitations. Frequently clinicians resort to a therapeutic trial of bile acid sequestrants, but this approach cannot provide a definitive diagnosis of bile acid malabsorption[5].

For these reasons, a novel MRI approach was conceived to measure bile acid transport and distribution *in vivo* using innovative multi-fluorinated bile acids (MFBA-MRI). MFBA containing three atoms of fluorine (^{19}F), a stable isotope of 100% natural abundance, are transported similarly to native bile acids[12], and can be used to visualize bile acid transport with a combination of proton (^{1}H) and fluorine (^{19}F) MRI, a sensitive, safe method without ionizing radiation exposure[13,14].

Protocol

The following protocol adheres to guidelines approved by the Institutional Animal Care and Use Committee (IACUC) at the University of Maryland School of Medicine (IACUC Protocol #0415011, approved June 18, 2015).

1. Gavaging Mice with ^{19}F-Labeled Bile Acids

1. Gavage mice with 150 mg/kg body weight ^{19}F-labeled bile acids. Fill a 1-ml syringe to the necessary volume with ^{19}F-labeled bile acid stock solution [cholic acid-trifluoro-acetyl lysine (CA-lys-TFA; in 1:1 polyethylene glycol 400:Dulbecco's phosphate buffered saline) or cholylsarcosine-trifluoro-N-methyl-acetamide (CA-sar-TFMA; in 60% polyethylene glycol 400 and 40% Dulbecco's phosphate buffered saline] and attach a 20-gauge 1.5-inch curved bulb-tipped gastric gavage needle. Make sure the gavage needle is long enough to reach the level of the mouse's xyphoid cartilage when inserted in the esophagus up to the hub of the needle
2. Firmly grasp the animal by the loose skin at the back of the neck between the thumb and index finger and use the remaining fingers to grasp the skin on the lower back and tail.

3. Hold the mouse upright and pass the gavage needle along the side and the roof of the mouth into the esophagus and down into the stomach. If resistance is encountered at the pharynx, reposition the needle until the animal 'swallows' it — do not push against resistance.
4. If anesthesia is required for gavage, place the mouse in a bell jar containing 5 ml isoflurane and close. When the mouse falls on its side, wait 7 sec, remove the mouse and perform gavage. To protect personnel from anesthetic vapors, use the bell jar only in a fume hood.
5. Observe the animal recover from isoflurane in a few min.
   NOTE: Since isoflurane is metabolized by the liver, a fluorine signal emanating from intact drug or its metabolites excreted into the biliary system and gallbladder can confound fluorine signals from ^{19}F-labeled bile acids[15]. An alternative is to use ketamine plus xylazine (see section 3.1 for doses).

2. Harvesting the Gallbladder, the Liver and Blood for Bile Acid Measurements Using Liquid Chromatography/Mass Spectrometry

1. To achieve maximal gallbladder filling, fast mice for at least 6 hr before harvesting the organs. Prepare ketamine and xylazine in phosphate-buffered saline (100 µl ketamine, 62.5 µl xylazine, 840 µl PBS).
2. Using a 1-ml sterile syringe, inject a mouse subcutaneously 1 hr prior to organ harvest with 15 µl/g body weight of ketamine/xylazine solution (150 mg ketamine and 18 mg xylazine per kg body weight).
3. One hr after administering ketamine/xylazine confirm adequate anesthesia by toe pinch and place the anesthetized mouse supine.
4. Use 5 or 6 inch scissors to make a midline abdominal skin incision from the pubis to the xyphoid and fine scissors (4 inch) to cut the peritoneal lining and expose abdominal organs — do not to pierce the diaphragm.
5. Grasp the xyphoid process with a 5 inch clamp and lift back across the chest to expose the upper abdominal cavity. Use forceps and a blunt instrument to dissect and move the liver aside, exposing the gallbladder.
   NOTE: Do not lacerate the liver or touch the gallbladder as the former will cause severe bleeding and the latter may stimulate gallbladder contraction and emptying.
6. Place a 4-inch clamp across the common bile duct (**Figure 3,** dashed arrows). Cut the ligament attaching the superior pole of the gallbladder to the diaphragm and gently move the gallbladder to the right side of the abdomen.

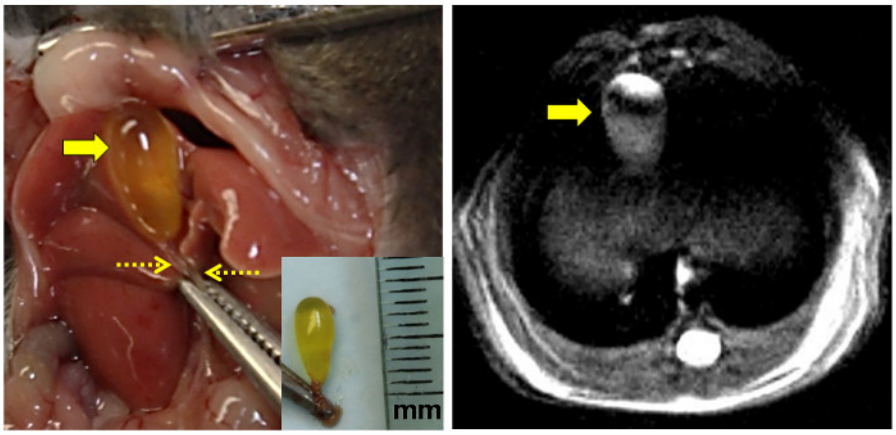

Figure 3: Anatomical and Proton MRI Views of the Mouse Gallbladder.
The left panel shows the exposed mouse gallbladder to the left of midline after abdominal incision. The clamp grasps the xyphoid process. The bile-filled fasting gallbladder is indicated by the large arrow and the clamped common bile duct by the dashed arrows. [*Inset:* Excised intact gallbladder with the common bile duct clamped. The ruler is marked in millimeters (mm).] The right panel shows a high-resolution proton density-weighted MRI image of the fasting murine gallbladder (arrow). Please click here to view a larger version of this figure.

7. Before excising the gallbladder perform cardiac puncture, harvest blood, and exsanguinate the animal to verify euthanasia.
   NOTE: Harvesting the gallbladder first may lacerate the liver causing cardiovascular collapse and failure to obtain an adequate blood sample (≥ 200 µl).
8. Expose the underside of the left diaphragm and identify the beating surface of the heart. At the point of maximal cardiac pulsation puncture the diaphragm and heart with a 23-gauge needle attached to a 1-ml syringe.
   1. Slowly withdraw the syringe while aspirating. When blood starts to fill the syringe, stop withdrawing and maintain suction to collect 0.2 - 0.6 ml blood. Gently rotating the needle or withdrawing it slightly may re-establish flow if it ceases.
   2. Transfer the blood to a 1.5-ml heparinized tube and centrifuge at 2,000 x g for 15 min. Precipitate the plasma with four parts acetonitrile and centrifuge at 12,000 x g for 10 min. Analyze the supernatant by liquid chromatography/mass spectroscopy (LC/MS/MS)[11-1312-1412-1412-1412-14]. If necessary, store the plasma at -80 °C before analysis.
9. Using blunt dissection, free the gallbladder from the liver. Transect the common bile duct below the clamp, remove and weigh the gallbladder, and place it in a 1.5-ml microcentrifuge tube. Harvest the liver.
10. Homogenize approximately 100 mg of liver and the entire gallbladder on ice in a size-21 glass tissue homogenizer. Extract with 75% acetonitrile and 25% water (800 µl for liver, 300 µl for gallbladder) and centrifuge at 12,000 x g for 10 min. Dilute extracts as necessary and quantify bile acid contents using LC/MS/MS[11-13].

3. Live Animal Proton (^{1}H) and Fluorine (^{19}F) Magnetic Resonance Imaging

1. To achieve maximal gallbladder filling, fast mice for at least 6 hr before imaging. Using ketamine and xylazine, anesthetize mice to prevent motion in the MRI scanner. Prepare a stock solution of ketamine plus xylazine in phosphate buffered saline (130 µl ketamine, 42.5 µl xylazine, 827 µl PBS). One hr before MRI, use a 1-ml sterile syringe to inject a mouse subcutaneously with 5 µl/g body weight of this solution (65 mg ketamine and 4.25 mg xylazine per kg body weight). To prevent dryness under anesthesia apply veterinary ointment to the animal's eyes.
2. After induction with ketamine/xylazine as above, clip a 1.5 cm^2 area on left lower half of the mouse abdomen using #40 or finer electric clipper blades. After fur removal, prep the area with 8 - 12% diluted iodine surgical scrub solution and rinse with 70% alcohol — repeat both steps. Insert a 24-gauge by 0.75-inch needle/catheter subcutaneously and tunnel into the abdominal cavity. Make sure the catheter is not in the cecum or other abdominal organ by pulling back on the plunger — there should be no blood or fecal material in the catheter.
3. Remove the needle and leave the intraperitoneal catheter. Place the mouse on a temperature-controlled thermal pad in the MRI scanner animal chamber.
4. Prepare a 1-ml sterile syringe containing ketamine and xylazine in phosphate buffered saline (1,000 µl ketamine, 300 µl xylazine, 6,700 µl PBS) and fill the desired length of 72-inch sterile tubing. Connect the intraperitoneal catheter to the prefilled sterile tubing and extend it away from the MRI scanner. To maintain anesthesia inject 50 µl of this solution every 20 min if the mouse's vital signs are stable.
   NOTE: Before imaging, make certain no metals are near the MRI scanner.
5. Use a ^{19}F/^{1}H dual-tuned linear volume MRI coil to transmit and receive radio frequency signals at 300.283 MHz for ^{1}H and 282.524 MHz for ^{19}F nuclei.
   1. Perform system calibration[11, 13] and animal localization with three-slice (axial, mid-sagittal, and coronal) scout images using a fast low-angle shot sequence (FLASH). To start the experiment, click the 'traffic light' button in the Scan Control window on the software console.
   2. Acquire multislice ^{1}H MR images using rapid acquisition with relaxation enhancement (RARE) sequence in the cross view of the sample or the body of the animal with repetition time 2,200 msec, echo time 8.9 msec, RARE factor 8, field of view 4 x 4 cm^2, slice thickness 1.0 mm, matrix size 266 x 266, in-plane resolution 150 x 150 μm^2, and number of averages 6. To start the experiment, click the 'traffic light' button in the Scan Control window on the software console.
   3. Acquire ^{19}F images using a FLASH sequence in the same region of the ^{1}H MRI with repetition time 220 ms, flip angle = 30°, echo time 3.078 ms, matrix size 32 x 32, in-plane resolution 1.25 x 1.25 mm^2, slice thickness 4.0 mm, and number of averages 768. To start the experiment, click the 'GOP' (**G**o- **O**n- **P**ipeline) button in the Spectrometer Control Tool window on the software console.
6. After MRI, euthanize the mouse with intraperitoneal injection of 15 µl/g body weight ketamine/xylazine solution (150 mg ketamine/18 mg xylazine per kg body weight) followed by cardiac puncture for exsanguination.
7. To recover a mouse from anesthesia, remove the intraperitoneal catheter but do not leave the animal unattended until it regains sufficient consciousness to maintain sternal recumbency.
8. To measure ^{19}F-labeled bile acid concentrations[11-13] from organ harvest, maintain anesthesia with ketamine plus xylazine as described above.

Representative Results

The use of MFBA for *in vivo* MRI to 'see' bile acid transport in real time has great potential for both research and clinical use. Moreover, the methods described here for resection of the gallbladder and biochemical analysis of its contents using liquid chromatography and mass spectrometry provide a means of confirming imaging results. However, the validity of these methods requires precise dosing, timing of assays, and localization of the gallbladder for imaging or surgical removal. For the latter, it is very important that the mouse's abdominal organs be perturbed as little as possible; even gentle manipulation of the gallbladder can stimulate contraction and emptying. Hence, to capture its entire contents, it is critical to place the clamp across the common bile duct as soon as possible.

Using the surgical approach suggested here, the gallbladder should be readily identified behind the right anterior lobe of the liver in the right upper quadrant of the abdomen (**Figure 3**). Moving the liver aside, without touching the gallbladder exposes the common bile duct for clamping. Once this clamp is in place, there should be no difficulty proceeding with the other steps described in the Protocol to remove the gallbladder intact.

The data in **Table 1** reveal highly selective concentration of MFBA in the gallbladder[13,14]. Organ (liver and gallbladder) concentrations of MFBA were calculated by assuming a density of 1 g/ml[13,14]. Within 7 hr of oral dosing, average accumulation of MFBA in the gallbladder was several orders of magnitude (1,000-fold) higher than that observed in either the liver or blood[13,14]; millimolar levels were observed in the gallbladder versus micromolar levels in liver and blood (**Table 1**). Average MFBA concentrations ranged from 0.4 - 1.4 µM in blood, 14.5 - 78.8 mM in liver, and 18.4 - 27.0 mM in gallbladder. These findings are consistent with MFBA being handled the same as physiological bile acids; after oral dosing, MFBA are actively transported by ASBT into the enterohepatic circulation whereby they are carried to the liver for active transport into hepatocytes by the sodium/taurocholate co-transporting polypeptide (NTCP), and excreted into the biliary tree for concentration in the gallbladder (**Figure 1**).

Figure 4 shows time-dependent accumulation of the ^{19}F signal in the gallbladder after gavage with MFBA. A more detailed time-course using analytical methods (LC/MS/MS) indicated that peak gallbladder concentrations of MFBA were observed in the range of 4 to 7 hr after oral dosing[12], a finding consistent with the physiological kinetics of enterohepatic circulation of bile acids. The left panel in **Figure 4**, an MRI image acquired two and one-half to four hr after oral gavage with MFBA, reveals ^{19}F signal emanating from what appears to be the common bile duct (dashed arrow) and a more robust signal emanating from the gallbladder (arrow); by 7 to 8.5 hr, the common bile duct signal is no longer detected and the gallbladder ^{19}F signal has increased to the same intensity as that emanating from the adjacent MFBA phantom (**Figure 4**, right panel, arrow).

We used mice with deficient expression of Asbt to test the ability of MFBA-MRI to detect reduced intestinal uptake of bile acids. As illustrated in **Figure 5A,** an approximately 22-fold reduction in the concentration of MFBA in gallbladder from Asbt-deficient mice was measured by LC/MS[13,14]; based on these findings it was anticipated that the MFBA ^{19}F MRI signal in these animals would be below the limits of detection. Indeed, as shown in **Figure 5B**, whereas a robust ^{19}F signal emanating from the gallbladder was detected in a wild-type mouse, there was no corresponding ^{19}F signal in the Asbt-deficient mouse[13,14]. These findings confirm that MFBA are handled similarly to physiological bile acids and that MFBA-MRI can be used to detect impaired intestinal uptake of bile acids.

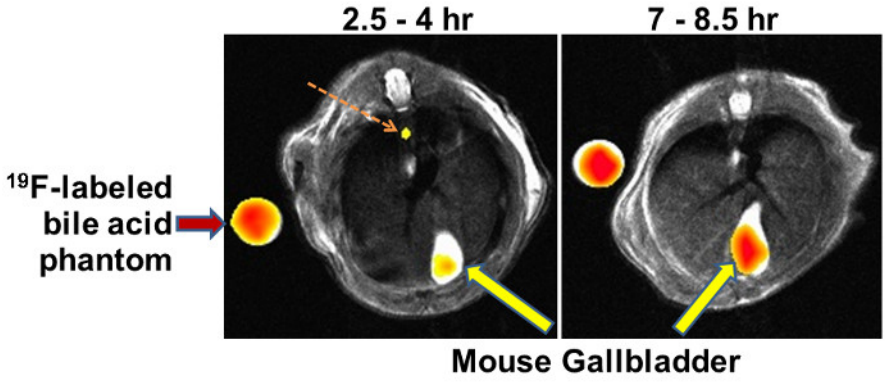

Figure 4: Representative MFBA-MRI Images.
Results of experiments in live mice show reconstruction overlays of ^{19}F and ^{1}H images demonstrating that ^{19}F signals emanate from the murine gallbladder (large arrows). Reference phantoms containing known concentrations of ^{19}F-labeled bile acids were placed in the MRI scanner alongside the mouse (left arrow). In the left panel, the dashed arrow indicates ^{19}F-labeled bile acid signal emanating from the common bile duct. Recorded above each panel is the time after gavage with ^{19}F-labeled bile acid that MRI was started to the time that image acquisition was completed (1.5 hr). As anticipated, gallbladder filling with the ^{19}F-labeled bile acid increases with time. Please click here to view a larger version of this figure.

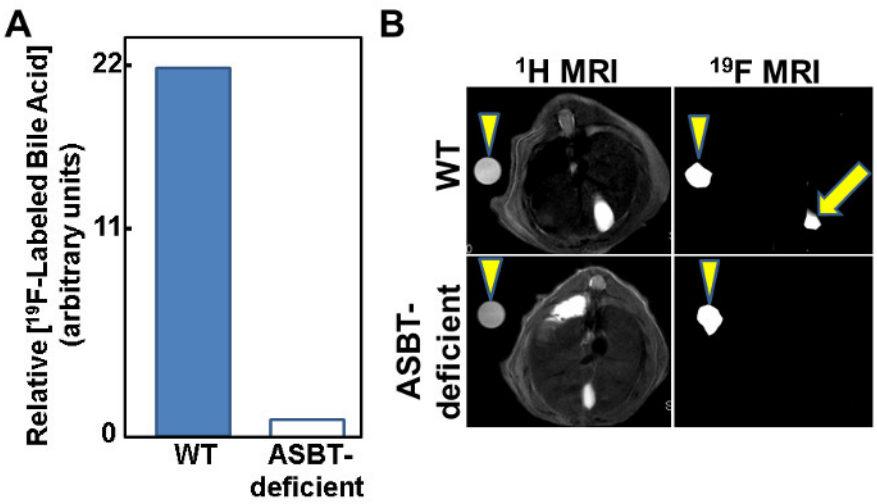

Figure 5: Attenuated MFBA-MRI Signal from Gallbladders of Asbt-deficient Mice.
(**A**) Bar graph illustrates that the concentration of MFBA measured by LC/MS/MS is approximately 22-fold lower in Asbt-deficient mice compared to control mice. (**B**) Absent MFBA-MRI signal from the gallbladder of an Asbt-deficient mouse. Arrowheads indicate ^{19}F-labeled bile acid phantoms (left panels) and ^{19}F MRI signal from phantoms (right panels). Arrow in upper right panel indicates ^{19}F-labeled bile acid signal emanating from the gallbladder; there is no corresponding ^{19}F-labeled bile acid signal in the Asbt-deficient mouse (lower right panel). Please click here to view a larger version of this figure.

	Gallbladder Weight (mg)	MFBA Concentration		
		Gallbladder (mM)	Liver (µM)	Plasma (µM)
CA-lys-TFA	25.2 ± 3.2	27.0 ± 2.4	78.8 ± 35.1	0.4 ± 0.2
CA-sar-TFMA	29.2 ± 2.4	18.4 ± 1.6	14.5 ± 0.6	1.4 ± 0.1

Table 1: Representative Values for Gallbladder, Liver and Plasma Concentrations of ^{19}F-labeled Bile Acids.
Mean ± standard error (SE) values are shown for gallbladder weight and the concentrations of the indicated MFBA in the gallbladder, liver, and plasma[12,13]. The values shown were measured 5 to 7 hr after gavaging mice with 150 mg/kg body weight of the indicated MFBA. Note the millimolar concentrations of MFBA in the gallbladder compared to micromolar concentrations in the liver and plasma. N = 3 mice per value for CA-lys-TFA and 5 mice per value for CA-sar-TFMA.

Discussion

The synthesis of CA-lys-TFA and CA-sar-TFMA and the *in vitro* analysis of their transport using stably transfected Madin-Darby canine kidney cells expressing ASBT and human embryonic kidney cells expressing the sodium/taurocholate co-transporting polypeptide (NTCP) are detailed elsewhere[13,14]. Here, the focus is on oral administration of MFBA by gavage to live animals, followed by harvest of the gallbladder, liver, and blood for analysis of MFBA content, and, notably, imaging MFBA in the gallbladder by live-animal MRI. Critical steps include avoiding fluorine-based anesthetics which may create competing ^{19}F signals, avoiding gallbladder manipulation before clamping the common bile duct which may result in gallbladder contraction and emptying before the organ is excised, and avoiding the placement of metals near the MRI scanner.

As detailed here and elsewhere[13,14], MFBA-MRI has great potential to successfully analyze bile acid transport *in vivo* under both normal and abnormal physiological conditions. Major strengths of MFBA-MRI are that it involves no ionizing radiation (neither MFBA labeled with naturally occurring, non-radioactive fluorine nor MRI emit ionizing radiation) and MFBA are administered orally without requiring venipuncture (unlike mice, most humans will not require parenteral administration of anesthetics or sedatives to prevent motion artifact in the MRI scanner). Substitution of a hydrolyzable bile acid with a synthetic bile acid resistant to hydrolysis by the gut microflora[13,14], can overcome issues regarding the *in vivo* stability of MFBA in the gut. The initial prototype for MFBA involved adding three fluorine atoms per molecule of cholic acid, a naturally occurring human bile acid that is hydrolyzed in the gut by *Clostridial* hydrolases[13,14]. A novel tri-fluorinated bile acid, CA-sar-TFMA, based on a sarcosine backbone that is resistant to hydrolysis by bacterial enzymes circumvented this limitation, extending the half-life of MFBA[13,14].

Lastly, a potentially competing methodology, the use of N-methyl-[^{11}C]cholylsarcosine for PET/CT, is limited by radiation exposure from both the radiolabeled bile acid and CT, and the need to prepare, ship, and store the radioactive bile acid[17].

Regarding modifications and troubleshooting for this novel methodology, one may consider that failure to detect an MRI signal emanating from the gallbladder may be due to a problem with the ^{19}F-labeled bile acid or its bioavailability, the timing of image acquisition, or insufficient filling of the gallbladder. As discussed above, we test the structural integrity of these agents by their ability to be transported *in vitro* by cell lines expressing the appropriate bile acid transporters. We allow at least 1.5 hr for image acquisition but in certain cases this duration may require extension. We find that fasting mice pre-MRI to ensure maximal gallbladder filling is important.

The limits of detection for ^{19}F-MRI signals require animal imaging for 90 - 120 min for adequate signal acquisition; this is likely too long for a practical clinical test - patients would have to lie still in the MRI scanner for that duration. Also, current, clinical MRI relies primarily on proton (^{1}H) imaging; the application of fluorine (^{19}F) imaging will require investment in hardware (^{19}F coil) and software, at least a $250,000 investment per MRI scanner. Until other fluorine-based MRI applications are developed using MFBA-MRI to evaluate patients for bile acid malabsorption is not likely to be cost-effective.

MFBA-MRI provides a promising alternative to measuring ^{75}SeHCAT retention, plasma 7α-hydroxy-4-cholesten-3-one (C4), and plasma FGF19, or performing a therapeutic trial using bile acid binders. In the U.S., ^{75}SeHCAT testing, which involves radiation exposure, is not FDA-approved. C4 and FGF19 testing has low positive-predictive value and testing is currently available only through specialized labs. Moreover, both C4 and FGF19 levels reflect hepatic synthesis of bile acids. Hence, unlike MFBA-MRI, these tests cannot detect altered expression or mutation of ileal bile acid transporters or other mechanisms of bile acid malabsorption that are independent of increased bile acid synthesis. Therapeutic trials of bile acid binders may be helpful but have uncertain predictive value and cannot provide a definitive diagnosis of bile acid malabsorption[5]. Finally, although direct measurement of fecal bile acids is seemingly reasonable this was rejected years ago as too cumbersome, impractical, and unreliable for routine clinical use[5].

Additional challenges must be overcome so that this innovative approach can be translated to measuring *in vivo* bile acid transport in the clinic (*e.g.*, for the diagnosis of bile acid malabsorption as a cause of chronic diarrhea). A major challenge is to maximize signal intensity by increasing the number of ^{19}F atoms per bile acid molecule without disrupting the ability of MFBA to behave like natural bile acids, that is, a bile acid molecule that is too bulky because of added ^{19}F atoms will not be transported by either ASBT or bile acid transporters in the liver. The ability of novel MFBA to be transported *in vitro* can be tested in cell lines expressing key human bile acid transporters[13,14] and should be predictive of *in vivo* transport. With increased sensitivity, MFBA-MRI has potential for improved imaging of the entire biliary tree (*e.g.,* common bile duct and its branches); in this regard, the ability to image the common bile duct in some mice appears promising (**Figure 4**, left panel).

Although the current limits of bile acid detection by MFBA-MRI allow their visualization only in the gallbladder, assuming the sensitivity of the technique can be improved we anticipate MFBA-MRI could be used to measure bile acid transport and distribution *in vivo* thereby providing comprehensive spatial information anatomically in real time; an enabling technology that would advance molecular imaging. MFBA-MRI would also offer a novel technology to assess the effects of gene polymorphisms and drugs that impair bile acid transporter function. MFBA-MRI has translational potential to help clinicians screen for bile acid malabsorption and thereby identify and manage illnesses resulting from increased fecal bile acids (*e.g.*, diarrhea that mimics irritable bowel syndrome). Lastly, should this technique becomes clinically available it has great

promise to accelerate progress in precision medicine by providing the capability to identify altered intestinal bile acid uptake in persons with colon neoplasia or other conditions that may be affected by changes in fecal bile acids.

Disclosures

The authors have nothing to disclose.

Acknowledgements

This work was supported by the National Institutes of Health, National Institute of Diabetes and Digestive and Kidney Diseases (grant numbers R21 DK093406 and T32 DK067872 to J-P.R.) and a VA Merit award (grant number 1BX002129 to J-P.R.).

References

1. Thomas, C., Pellicciari, R., Pruzanski, M., Auwerx, J., & Schoonjans, K. Targeting bile-acid signalling for metabolic diseases. *Nat Rev Drug Discov.* **7**, 678-693 (2008).
2. Vallim, T. Q., & Edwards, P. A. Bile acids have the gall to function as hormones. *Cell Metab.* **10**, 162-164 (2009).
3. Dawson, P. A., & Karpen, S. J. Thematic Review Series: Intestinal Lipid Metabolism: New Developments and Current Insights Intestinal transport and metabolism of bile acids. *Journal of Lipid Research.* **56**, 1085-1099 (2015).
4. Dawson, P. A. *et al.* Targeted deletion of the ileal bile acid transporter eliminates enterohepatic cycling of bile acids in mice. *J Biol Chem.* **278**, 33920-33927 (2003).
5. Pattni, S., & Walters, J. R. Recent advances in the understanding of bile acid malabsorption. *Br Med Bull.* **92**, 79-93 (2009).
6. Walters, J. R. *et al.* A new mechanism for bile acid diarrhea: defective feedback inhibition of bile acid biosynthesis. *Clin Gastroenterol Hepatol.* **7**, 1189-1194 (2009).
7. Hofmann, A. F., Mangelsdorf, D. J., & Kliewer, S. A. Chronic diarrhea due to excessive bile acid synthesis and not defective ileal transport: a new syndrome of defective fibroblast growth factor 19 release. *Clin Gastroenterol Hepatol*. **7**, 1151-1154 (2009).
8. Flynn, C. *et al.* Deoxycholic acid promotes the growth of colonic aberrant crypt foci. *Mol Carcinog.* **46**, 60-70 (2007).
9. Glinghammar, B., & Rafter, J. Carcinogenesis in the colon: interaction between luminal factors and genetic factors. *Eur J Cancer Prev*. **8 Suppl 1**, S87-94 (1999).
10. Bernstein, C. *et al.* Carcinogenicity of deoxycholate, a secondary bile acid. *Arch Toxicol.* **85**, 863-871 (2011).
11. Zheng, X., Ekins, S., Raufman, J. P., & Polli, J. E. Computational models for drug inhibition of the human apical sodium-dependent bile acid transporter. *Mol Pharm*. **6**, 1591-1603 (2009).
12. Vivian, D. *et al.* Design and characterization of a novel fluorinated magnetic resonance imaging agent for functional analysis of bile Acid transporter activity. *Pharm Res.* **30**, 1240-1251 (2013).
13. Vivian, D. *et al.* Design and evaluation of a novel trifluorinated imaging agent for assessment of bile acid transport using fluorine magnetic resonance imaging. *J Pharm Sci*. **103**, 3782-3792 (2014).
14. Vivian, D. *et al.* In vivo performance of a novel fluorinated magnetic resonance imaging agent for functional analysis of bile acid transport. *Mol Pharm*. **11**, 1575-1582 (2014).
15. Raufman, J. P. *et al.* In Vivo Magnetic Resonance Imaging to Detect Biliary Excretion of 19F-Labeled Drug in Mice. *Drug Metab Dispos.* **39**, 736-739 (2011).
16. Ridlon, J. M., Kang, D. J., & Hylemon, P. B. Bile salt biotransformations by human intestinal bacteria. *J Lipid Res.* **47**, 241-259 (2006).
17. Frisch, K. *et al.* [N-methyl-11C]cholylsarcosine, a novel bile acid tracer for PET/CT of hepatic excretory function: radiosynthesis and proof-of-concept studies in pigs. *J Nucl Med.* **53**, 772-778 (2012).

